

Vesicles in Poiseuille flow

Gerrit Danker¹, Petia M. Vlahovska², and Chaouqi Misbah¹

¹*Laboratoire de Spectrométrie Physique, UMR, 140 avenue de la physique, Université Joseph Fourier, and CNRS, 38402 Saint Martin d'Heres, France*

²*Thayer School of Engineering, Dartmouth College, 8000 Cummings Hall, Hanover NH 03755, USA**

(Dated: March 8, 2009)

Blood flow in the microcirculation depends crucially on the migration of red blood cells towards the flow centerline. We develop an analytical theory that sheds light on the migration mechanisms. Our results identify the ratio of the inner over the outer fluid viscosities λ as the main controlling parameter; the membrane bending resistance is of less importance. At low λ , the vesicle deforms into a tank-treading shape, which is an ellipsoid if the vesicle is far-away from the flow centerline. The resulting migration is always towards the flow centerline, unlike other soft particles such as drops. Above a critical λ , the vesicle tumbles and cross-stream migration is suppressed. The theory predicts a surprising coexistence of two types of shapes at the centerline, a bullet-like and a parachute-like shape.

PACS numbers: 87.16.Dg 83.50.Ha 87.17.Jj f3.80.Lz 87.19.Tt

Keywords:

Blood is a complex fluid composed primarily of red blood cells (RBCs) suspended in water with volume fraction about 45%. The relation between blood microstructure and flow is a long-standing problem in circulatory research [2, 3]. A phenomenon that has received considerable attention is the decrease of apparent blood viscosity in small vessels with diameter $< 500\mu m$ (Fahraeus–Lindqvist effect). This has been linked to the formation of a cell-free layer near the walls due RBCs migration towards the flow centerline, first observed by Poiseuille. Cross-stream particle motion can result from (1) hydrodynamic repulsion by the wall, and (2) shear-rate gradients in pressure-driven (quadratic) flows, which tend to drive deformable particles towards regions with lower shear in order to minimize shape distortion [4]. The latter effect becomes dominant in blood vessels such as arterioles, which are 10-50 times larger than the cells. Given that the RBC diameter is about $8\mu m$, the shear-gradient effects are expected to be significant in blood vessels with diameter in the range $100 - 500\mu m$. In such cases, a cell that is few diameters away from the centerline feels mainly the flow curvature, not the walls. Despite its importance, the effect of flow curvature on RBC dynamics has been considered only to a limited extent [5, 6].

Giant vesicles made of pure bilayer membranes mimic essential features of the RBC such as its equilibrium bi-concave shape, tank-treading (see below) and tumbling under shear flow. Thus, vesicles have gained popularity as well-defined models to study the RBC mechanics. Recent studies have highlighted that the unique mechanical properties of the lipid bilayer membrane, such as fluidity, incompressibility and resistance to bending, give rise to a number of fascinating nonequilibrium features of the vesicle and RBC micro-hydrodynamics. For example, in

linear flows vesicles and RBCs exhibit amazing variety of motions [7–9]: (i) tank-treading (TT) (the fluid membrane rotates as a tank-tread, while the orientation angle of the vesicle remains fixed in time), (ii) tumbling (TB), (iii) vacillating-breathing (VB) (the long axis undergoes oscillation about the flow, while the shape shows breathing) [10], called alternatively swinging [11]. These dynamics have strong impact on rheology [12].

The complex behavior of vesicles in linear flow hints at even more intricate dynamics in quadratic flows, which we explore in this Letter. More specifically we address open questions such as: What is the role of flow curvature in cross-stream vesicle and RBC migration? Is there relation between the migration direction and the basic modes of vesicle and RBC dynamics (i.e. TT, VB and TB)? What physical parameters control vesicle and RBC migration? A theory that can answer these questions represents a challenging problem because not only the shape, but also the location of the vesicle is not known a priori, and it must be solved for in a consistent manner. The development of the theory and the resulting physical insights are reported in this Letter.

Let us consider a vesicle placed in a plane Poiseuille flow, i.e., a pressure-driven flow bounded by two parallel infinite plane walls. In a reference frame centered in the vesicle, the ambient flow is written as

$$\mathbf{v}_0 = (-v_s - \dot{\gamma}y - \alpha y^2) \mathbf{e}_x, \quad (1)$$

where α is a measure of the curvature of the flow profile, $\dot{\gamma}$ is the local shear rate, which depends to the distance between the vesicle center and the flow axis, y_0 , $\dot{\gamma} = 2y_0\alpha$, and v_s is the (still undetermined) slip velocity, which is the difference between the actual velocity of the vesicle center in the flow direction and the velocity of the unperturbed flow.

The flow about the vesicle is described by the Stokes equations, because at the length scales of the vesicle vis-

*chaouqi.misbah@ujf-grenoble.fr

cosity dampens fluid acceleration. The velocity, \mathbf{v} , and the pressure, p , fields satisfy

$$\nabla p = \eta_i \nabla^2 \mathbf{v}, \quad \nabla \cdot \mathbf{v} = 0, \quad (2)$$

where η_1 is the viscosity of the fluid encapsulated by the vesicle and η_2 is the viscosity of the suspending medium; $\lambda \equiv \eta_1/\eta_2$ measures the viscosity ratio.

Assuming a nearly spherical shape, the time-dependent vesicle configuration is described by

$$\mathbf{R} = \mathbf{R}_0 + r_0[1 + \epsilon f(t, \theta, \phi)] \mathbf{e}_r, \quad (3)$$

where $\mathbf{R}_0 = (x_0, y_0, z_0)$ is the time-dependent position of the centroid of the vesicle and f describes shape deviation from the spherical shape, with ϵ a small parameter (see below). θ and ϕ are the spherical coordinates, and r_0 is the radius of a sphere having the same volume as the vesicle. The vesicle shape $f(\theta, \phi)$ can be decomposed in an infinite series of spherical harmonics $Y_{lm}(\theta, \phi)$

$$f = \sum_l f_l = \sum_l \sum_{m=-l}^l F_{lm}(t) Y_{lm}(\theta, \phi). \quad (4)$$

$F_{lm}(t)$ describes the shape evolution. The imposed flow (1) can be represented as a superposition of fundamental solutions of the Stokes equation that involve vector spherical harmonics of order 1, 2, and 3. Thus, it is sufficient, to leading order, to include the $l = 0$ mode, which ensures volume conservation, and the $l = 1, 2, 3$ modes.

The solution to (2) is obtained as an expansion, $\mathbf{v} = \mathbf{v}^{(0)} + \mathbf{v}^{(1)}(f) + \dots$, in the excess area, which is the difference in the areas of the vesicle and that of a sphere with the same volume, i.e., $\Delta = A/r_0^2 - 4\pi \sim f^2$. A small deformation theory is expected to be valid for $\Delta < 1$. From the definition of the area it is evident that Δ is a quadratic function of the shape deviation from sphere. Thus it is convenient to set $\epsilon = \Delta^{1/2}$ as the formal expansion parameter. The velocity field is given by the classical Lamb solution [13]. This solution contains integration factors which are determined from the boundary conditions. These are: (i) Continuity of the fluid velocity across the membrane (valid if impermeability is assumed). (ii) Continuity of the stress across the membrane: the jump of fluid stress across the membrane is balanced by the membrane force. The latter consists of a normal force due to resistance to bending, and a tangential (fictitious) force, which originates from a Lagrange multiplier enforcing the area constraint. (iii) Local membrane incompressibility, which restricts the surface velocity field to be solenoidal. This approach has been successfully applied to solve for the vesicle dynamics in a linear flow [10, 13, 14, 16]. We have generalized the method to treat vesicles in quadratic flows. A new feature in the analysis is that, unlike linear flows, the vesicle center moves with different velocity than the ambient flow. This fact has to be carefully accounted for and leads to a kinematic condition for the vesicle translation

$$\dot{\mathbf{R}}_0 \cdot \hat{\mathbf{r}} \equiv \sum_{m=-1}^1 \partial_t F_{1m} Y_{1m} = (v_s \hat{\mathbf{x}} - \mathbf{v}^{(0)}) \cdot \nabla f, \quad (5)$$

where we have retained only the leading order terms, which are linear in the deformation f . $\mathbf{v}^{(0)}$ is the solution for the flow about a spherical vesicle in quadratic flow. Eq. (5) shows that migration arises from the interaction of the perturbed flow and the non-spherical, deformable vesicle shape. Details of the solution can be found in the supplementary material [1]; here we focus on the results and discuss the physical implications. Vesicles cross-stream migration occurs even at leading order and the migration direction is always towards the centerline, in contrast to drops [4]. Next we show that the migration velocity depends in a non-trivial way on the viscosity ratio and excess area.

The cross-stream migration along the y -direction is obtained from Eq. (5), $v_m = \partial_t F_{11} + \partial_t F_{1-1}$. It depends on the instantaneous shape

$$\begin{aligned} v_m = & \frac{i}{4} \sqrt{\frac{30}{\pi}} \alpha \epsilon r_0^2 \frac{36\lambda + 71}{(\lambda + 4)(76\lambda + 85)} (F_{22} - F_{2,-2}) \\ & + \frac{16}{7} \sqrt{\frac{21}{\pi}} \frac{\alpha \epsilon r_0 y_0}{23\lambda + 32} (F_{31} - F_{3,-1}) \\ & + \frac{48}{7} \sqrt{\frac{35}{\pi}} \frac{\alpha \epsilon r_0 y_0}{23\lambda + 32} (F_{33} - F_{3,-3}). \end{aligned} \quad (6)$$

At leading order, only the $l = 2, 3$ shape modes are excited by the ambient flow. Their time evolution is described by the following equations:

$$\epsilon \mathcal{D}_t F_{2m} = -\frac{24(\sigma_0 + 6\kappa)}{23\lambda + 32} F_{2m} + \frac{\alpha y_0}{23\lambda + 32} N_{2m}, \quad (7)$$

$$\epsilon \mathcal{D}_t F_{3m} = -\frac{120(\sigma_0 + 12\kappa)}{76\lambda + 85} F_{3m} + \frac{\alpha r_0}{76\lambda + 85} N_{3m} \quad (8)$$

with $\mathcal{D}_t = \partial_t + im\alpha y_0$, and $N_{20} = N_{2,\pm 1} = 0$, $N_{2,\pm 2} = \pm i 8\sqrt{30}\pi$, $N_{30} = N_{3,\pm 2} = 0$, $N_{3,\pm 1} = \mp 5\sqrt{21}\pi/3$, $N_{3,\pm 3} = \mp 5\sqrt{35}\pi$. κ is the membrane bending rigidity rescaled by $r_0^3 \eta_2/\epsilon$. We have checked that higher order terms in the evolution equations are not important for the migration in quadratic flow; these terms, however, were essential for the determination of the phase diagram (TT, TB and VB) in linear flows [15, 16]. A complete discussion will be reported elsewhere. The evolution equations (7, 8) contain the tension-like quantity σ_0 , which is the homogeneous part of the Lagrange multiplier [1, 13, 16]. Its value is computed from the condition that the shape deformation complies with the available excess area $\Delta = 2 \sum_{m=-2}^2 F_{2m} F_{2m}^* + 5 \sum_{m=-3}^3 F_{3m} F_{3m}^*$.

The excess area is redistributed differently among the shape modes depending on the distance to the centerline. Eqs. (7) and (8) show that if $F_{2m} \sim \Delta^{1/2}$ then $F_{3m} \sim r_0 \Delta^{1/2}/y_0$. Near the flow axis, $y_0 \sim r_0$, the excess area can be stored in both F_{2m} and F_{3m} modes, which hints at a possibility for multiple stationary shapes. Far from the centerline, $y_0 \gg r_0$, the linear component of the flow with shear rate $2y_0\alpha$ is large. Accordingly, the excess area is concentrated only in the ellipsoidal F_{2m} modes. Not surprisingly, for $\lambda < \lambda_c$, where λ_c is the viscosity

ratio for the TT to TB transition [10], a numerical solution of the coupled equations for the shape (7, 8) and the migration (6) yields the usual tank-treading ellipsoidal shape for the vesicle [10]. The interaction between the TT ellipsoid and the quadratic flow causes the migration towards the center of the flow, see Fig. (1). The

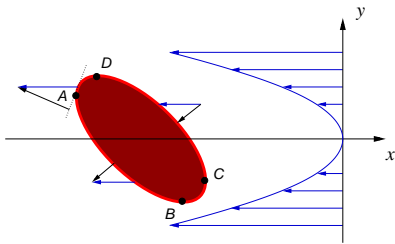


FIG. 1: (Color online) A vesicle in Poiseuille flow far from the centerline. The local velocity field can be decomposed into a local shear $\dot{\gamma}(y_0)$ (responsible for the tank-treading vesicle at the shown orientation) and a (small) quadratic correction (blue arrows). Due to the inclination of the vesicle long axis with respect to the quadratic flow field, there is a net force acting on the vesicle in the negative y direction.

quadratic correction $-\alpha y^2$ acting on the membrane of the vesicle, can be decomposed into two components: one tangential to the membrane, which locally modifies the tank-treading velocity, and one normal to the membrane, which modifies the vesicle shape and possibly causes migration. In the segments AB and CD the perpendicular component tends to push the vesicle into the negative y direction, whereas in the smaller segments DA and BC , the perpendicular component pushes the vesicle in the positive y direction. As the segments AB and CD account for most of the vesicle's surface, the net force has a component in the negative y direction (towards the flow centerline). The corresponding migration velocity is

$$v_m = -\frac{17284\lambda^2 + 66671\lambda + 55840}{60(\lambda + 4)(23\lambda + 32)(76\lambda + 85)} \sqrt{\frac{30}{\pi}} \alpha \Delta^{1/2} r_0^2. \quad (9)$$

Note that even though the leading-order shape is described by the F_{2m} mode, both F_{2m} and F_{3m} modes contribute to the migration. For $\lambda \sim 1$ the migration velocity is approximately $v_y = -0.16 \alpha \Delta^{1/2} r_0^2$. In a typical experiment in a rectangular microchannel we have $\alpha \sim 0.3 (\mu\text{m}\cdot\text{s})^{-1}$, $\Delta = 0.25$, $r_0 = 20 \mu\text{m}$, and a migration velocity of $0.75 \mu\text{m}/\text{s}$ [17]. Using Eq. (9), we find an expected migration velocity of about $1 \mu\text{m}/\text{s}$. Note also that (9) is independent of the membrane bending rigidity. For large y_0 , the terms 6κ and 12κ in Eqs. (7, 8) become negligible compared to the tension terms. The tension σ_0 increases with the distance from the centerline as $\sigma_0 \sim y_0$, because the elongational component of the flow (with strength given by the local shear rate, $\dot{\gamma} \sim y_0$) must be compensated by the membrane tension in order to satisfy the local membrane incompressibility.

What happens if $\lambda > \lambda_c$? Far from the centerline, $y_0 \gg r_0$, the vesicle tumbles. In this case we have in-

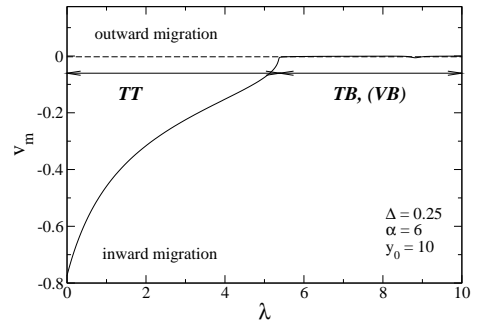


FIG. 2: Migration velocity as a function of the viscosity ratio λ for the various regimes: tank-treading (TT), tumbling (TB), and vacillating-breathing (VB).

tegrated numerically the set of equations (7,8,6). The migration (averaged over time) is again always towards the flow centerline but the magnitude of the migration velocity is very close to zero (of the order of $10^{-2} r_0$ per tumbling cycle). Due to TB, the up-down asymmetry, which is responsible for migration (Fig.1), is vanishingly small over a period of TB (note that the TB period is set by the local shear rate). This explains the small migration in the TB regime.

To summarize, for a given excess area, vesicle migration depends mainly on the viscosity ratio as illustrated on Fig.2. For large viscosity ratios, $\lambda \gg 1$, the migration velocity must go to zero, since the vesicle behaves as a rigid sphere. The kinematic reversibility of the Stokes equations precludes a cross-stream migration in this case. This feature is also evident from the expression for the migration velocity (6). Indeed, the F'_{ij} s are finite due to the constraint of fixed excess area, but the prefactors $O(\lambda^{-1})$. Thus, when $\lambda \rightarrow \infty$, $v_m \rightarrow 0$.

For a given viscosity ratio, the migration velocity is expected to depend non-monotonically on the excess area Δ . A spherical object (i.e., $\Delta = 0$) does not migrate, $v_m = 0$, due to the up-down symmetry. Deflated vesicle with high $\Delta \gtrsim 1$ readily tumbles because the critical viscosity ratio is low [10]; then we similarly expect $v_m \sim 0$. Hence, it follows that the absolute value of the migration velocity attains a maximum for a certain value of Δ (details will be reported elsewhere). This results also agrees with the argument given on the lift force under a linear shear flow [18], and with experiments [17].

Vesicle trajectories: Figure 3 shows that as the vesicle moves towards the centerline, its shape deforms more and more until it becomes a parachute (or assumes another shape, namely bullet-like, as discussed below) when the centerline is reached. If the ratio $\eta_0 r_0^4 \alpha / \kappa$ (this is a measure of the relative strength of hydrodynamic and bending stresses) is sufficiently large (typically above 10), the vesicle approaches the centerline monotonously. However, for smaller curvature of the flow field (or higher membrane rigidity) the vesicle trajectory exhibits damped oscillations about the centerline. For

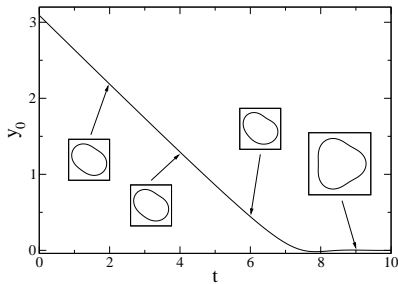


FIG. 3: Evolution of the vertical position of the vesicle as a function of time. Some snapshots of the vesicle shape along the trajectory are shown as insets. Parameters: $\alpha = 6$, $\kappa = 1$, $\Delta = 0.25$.

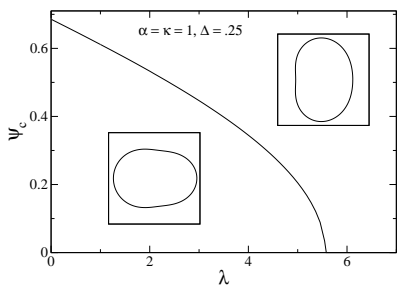


FIG. 4: Critical angle ψ_c separating the basins of attraction for two coexisting solutions at the centerline.

typical values $\alpha \sim 0.1(\mu\text{ms})^{-1}$, $r_0 \sim 10\mu\text{m}$ [17], viscosity of water, and $\kappa \sim 40k_B T$ [19], one finds that $\eta_0 r_0^4 \alpha / \kappa \sim 0.1$. Accordingly, these damped oscillations should be relatively easy to observe experimentally.

Vesicle shapes at the centerline: RBCs deform into parachute-like shapes when squeezed through narrow capillaries [5, 20], a direct consequence of the flow curvature. A new surprising feature we have discovered is the coexistence of two shape solutions at the centerline for small curvature of the flow field, see Fig. 4. This is a result from the nonlinear shape equations (7,8); recall that the tension is shape-dependent. We found two shape solutions if $\eta_0 r_0^4 \alpha / \kappa$ is lower than about 5. For one solution the longest axis of the vesicle is oriented in the flow direction (bullet-like shape), and for the other one it is perpendicular to it (parachute-like shape). Each of these solutions has its own basin of attraction, i. e., if the initial angle at the centerline is smaller than ψ_c , the bullet-like shape is attained, and otherwise the parachute-like shape. If, however, the curvature of the flow is large ($\eta_0 r_0^4 \alpha / \kappa > 5$), the vesicle assumes a pronounced parachute-like shape, and the two solutions are indistinguishable. Different morphology results in different slip velocity, which leads to different dissipation and flow resistance. The slip velocity for the parachute-like shape is higher, while for a bullet-like vesicle is lower than that of a rigid sphere, $v_s = -1/3 \alpha r_0^2$ (as deduced from Faxen's law [4]). We will report further on this matter in a future work. The parameter range where these shapes co-exist, $10^{-1} < \eta_0 r_0^4 \alpha / \kappa < 10$, is experimentally accessible [17]. This means that in principle this prediction is not devoid of experimental testability. Finally, the analysis has been also performed for a biologically more relevant axisymmetric flow and yields the same qualitative results for the migration direction, coexistence of two shapes, and small migration in the tumbling regime [1].

C.M. Acknowledge financial support from CNES and ANR (MOSICOB project).

-
- [1] supplementary material
[2] A. R. Pries and T. W. Secomb. *Clinical hemorheology and microcirculation*, 29:143–148, 2003.
[3] A. S. Popel and P. C. Johnson. *Annu. Rev. Fluid Mech.*, 37(1):43–69, 2005.
[4] L. G. Leal. *Ann. Rev. Fluid Mech*, 12:435–476, 1980.
[5] H. Noguchi and G. Gompper. *PNAS*, 102:14159–14164, 2005.
[6] B. Kaoui, G. H. Ristow, I. Cantat, C. Misbah, and W. Zimmermann. *Phys. Rev. E*, 77:021903, 2008.
[7] V. Kantsler and V. Steinberg. *Phys. Rev. Lett.*, 95:258101, 2005; *ibid* 96:036001, 2006.
[8] M.-A. Mader, V. Vitkova, M. Abkarian, A. Viallat, and T. Podgorski. *Eur. Phys. J. E*, 19:389–397, 2006.
[9] M. Abkarian and A. Viallat. *Soft Matter*, 4:653–657, 2008.
[10] C. Misbah. *Phys. Rev. Lett.*, 96:028104, 2006.
[11] H. Noguchi and G. Gompper, *Phys. Rev. Lett.* 98, 128103 (2007).
[12] G. Danker and C. Misbah, *Phys. Rev. Lett.* **98**, 088104 (2007).
[13] U. Seifert. *Eur. Phys. J. B*, 8:405–415, 1999.
[14] P. M. Vlahovska and R.S. Gracia. *Phys. Rev. E*, 75:016313, 2007.
[15] V. V. Lebedev, K. S. Turitsyn, and S. S. Vergeles. *Phys. Rev. Lett.*, 99:218101, 2007.
[16] G. Danker, T. Biben, T. Podgorski, C. Verdier, and C. Misbah. *Phys. Rev. E*, 76:041905, 2007.
[17] G. Couplier, B. Kaoui, T. Podgorski, and C. Misbah, *Phys. Fluids* **20**, 111702 (2008).
[18] P. Olla J. *Phys. II (France)* **7**, 1533 (1997); *Physica A* **278**, 87 (2000).
[19] *Structure and Dynamics of Membranes, Handbook of Biological Physics*, edited by R. Lipowsky and E. Sackmann (Elsevier, Amsterdam, 1995).
[20] R. Skalak and P. I. Branemark. *Science*, 164:717 – 719, 1969.